Hadronic deformation energy. II. Two-nucleon interaction*

Carleton DeTar†

Center for Theoretical Physics, Laboratory for Nuclear Science and Department of Physics, Massachusetts Institute of Technology, Cambridge, Massachusetts 02139

(Received 1 July 1977)

The MIT bag model for hadrons is treated in the static cavity approximation. The adiabatic deformation of a six-quark hadron with quantum numbers of the deuteron is studied in a configuration which permits the separation of two triplets with quantum numbers of the neutron and proton. The energy of the system is computed to second order in the gluon coupling and presented as a function of two choices of a single collective variable: a separation parameter for the nucleons and the baryonic quadrupole moment. The present study considers only interactions at short and intermediate range in a state with nuclear spins aligned in parallel along the deformation axis. It does not treat effects depending on nucleon momenta. The energy, when expressed in terms of a nuclear separation parameter, exhibits a soft repulsive core at short range due to a color-magnetic gluon interaction, and strong attraction in intermediate range due to a color-electric interaction.

I. INTRODUCTION

The two-nucleon force is probably the most studied of all hadronic interactions. Since it was first proposed in 1935, the Yukawa model of meson exchange[1] has served as the organizing principle for theoretical efforts to understand the two-nucleon interaction. Highly sophisticated models involving several meson species and multiple meson exchange have been proposed to account for the observed low-energy-scattering data.[2] However well these models succeed in accounting for the long-range aspects of the interaction, there is no reason to believe that their usefulness extends to short range; indeed practical models abandon theory and draw from experiment for information about the interaction in this regime.[3] Because of the extended nature of the nucleons, it is clear that at short distances a two-body wave function must fail to describe adequately the complexity of a two-nucleon system.

Present-day approaches to the understanding of the structure of the nucleon have progressed considerably from the early picture of a single elementary fermion surrounded by a cloud of mesons. Obviously our understanding of the two-nucleon interaction should keep abreast of these developments. Accordingly, we have taken a model which has been quite successful in accounting for the static properties of the light mesons and baryons, namely, the MIT bag model,[4] and have applied it in an effort to understand the short-distance interaction of the two-nucleon system.[5]

The MIT bag model describes hadrons in terms of the currently fashionable color-SU(3) gauge theory of quarks and gluons. These elementary constituents are confined to a finite volume by a uniform external pressure, a key innovation of the model. Taken in the static cavity approximation[6] the model is perhaps the only one currently available in which calculations of the type presented here are feasible.

In the static cavity approximation the nucleon is regarded as a collection of three quarks (we do not take into account mixing with states with gluons or extra quark-antiquark pairs) interacting via gluon exchange and confined to a volume with fixed walls. The two-nucleon interaction arises when two such cavities join and the quarks intermingle, altering the effects of gluon exchange. When the cavities are separated, no interaction occurs. Clearly, this approach can give no information about the long-range effects of pion exchange, for example, which presumably would be associated with a proper treatment of quantum surface fluctuations in which quark-antiquark pair creation is involved.[6] Thus we have devoted our attention to the short-range properties of the interaction. Here the cavity assumes a nearly spherical outline. Since this is also the shape which is assumed by the noninteracting hadrons, whose static properties have been studied with considerable success,[7] we trust that our computations will have comparable validity in this regime.

It is conceivable that the meson-exchange picture and the quark-interchange picture of the bag-model are complementary over some intermediate range. The quark-interchange diagram viewed from the point of view of the crossed channel appears as the exchange of a quark-antiquark pair, from which mesons are constructed. However, the correspondence between the crossed-channel spectrum and the direct-channel interaction energy is made obscure by the static cavity approximation.

The bag model, in present form, does not take

into account the process of creation and annihilation of the bags themselves. Thus what is obtained from the present calculation is more properly regarded as a potential from which a unitary scattering matrix is to be constructed.

Our approach to the two-nucleon interaction involves studying the adiabatic deformation of a bag containing six quarks into two bags containing three each. Normally the shape of the cavity is determined by the condition that the internal field pressure be a constant on the surface. Thus the ground state of the six-quark system in the static cavity approximation is, strictly speaking, the state of minimum energy which achieves this pressure balance. This state is the semiclassical deuteron, and in the present calculation it is a single nearly spherical cavity containing six quarks with a binding energy of ~190 MeV. However, quantum fluctuations about this minimum energy, in particular fluctuations altering the shape, modify both the energy and the description of the state. The approach we have adopted in order to follow these fluctuations is one quite analogous to that of the Born-Oppenheimer approximation for the interaction energy of two hydrogen atoms.[8] There, a single collective variable, namely, the internuclear separation is fixed and the orbital energy of the electrons is computed. What emerges is an effective central potential for a two-body system, which is then used to obtain vibrational and rotational levels of the hydrogen molecule. The justification for this approach lies in the notion that the nuceli, which are far more massive than the electrons, move with very small velocities compared to those of the electrons. Thus the impact of their motion upon the electron orbitals can be treated adiabatically and classically. In the present application there is no analog to the massive pointlike positive charges. However, it is felt that any gross collective variable which describes the bulk conformation of the six-quark system must vary slowly on a time scale characteristic of the motion of the essentially massless quarks. We have two criteria in mind which establish qualitative limits on this approximation: First, the cavity energies of the quarks must be small compared to the overall mass involved in the collective motion. Second, the kinetic energies involved in the collective motion must be small compared to this mass. We believe that these criteria are fulfilled in the two-nucleon system near threshold. However, considerable care would be needed in order to apply this method to resonance decays in which large kinetic energies are encountered, or to decays involving the π meson in which masses comparable to the quark-cavity energies are encountered.

We study the energy of the six-quark system as a function of the collective variable by fixing the expectation value of this variable by adding a constraint to the Hamiltonian:

$$H \to H - c_\theta \Theta$$

where c_θ is a Lagrange multiplier and Θ is the operator defining the collective variable. Two variables are chosen. One is a parameter which measures the separation of the three-quark systems. The second is the baryonic quadrupole moment. In order to interpret the resulting curves as representing potential energies some care must be exercised. First, one must find some way of splicing together the short-range information from the bag model and the long-range information from meson exchange. Second, one must deal with at least the rudimentary question of defining a mass parameter to be associated with the collective coordinate. This problem can be compared to advantage with the analogous problem in the theory of nuclear collective motion.[9] Presumably similar techniques would work here. The objective of such a study would be to obtain a probability amplitude at a given energy for a given value of the collective coordinate. Thus, for example, the deuteron would be regarded as a quantum superposition of states of a six-quark nature at close range and two-nucleon nature at long range. Whether a single collective variable suffices at close range or more than one must be considered is, of course, a question which must be kept in mind in future work.

The present work represents the first serious effort at applying a consistent model of confined quarks to the two-nucleon problem. It is not meant to be exhaustive. We have not studied the spin and isospin dependence of the interaction, although this can readily be done with similar methods. We do not study dynamical effects which would lead to a construction of the two-nucleon wave function and a determination of static properties of the deuteron. These questions are left to subsequent work. We explore here the details and subtleties of the model and use it as a theoretical laboratory in an attempt to isolate the important phenomena which control the interaction.

The details of the model and computational method are set forth in the previous article[10] (hereafter refered to as I). In the interest of completeness, a brief review of the construction of the effective Hamiltonian is given in Sec. II. The six-quark configuration is defined in Sec. III and the computation of the "configuration factors" of the effective Hamiltonian is described in the Appendix. The only essential difference between the computation for the quark-antiquark state in I and the

six-quark state appears in the configuration factors. A two-orbital approximation to the cavity Lamb shift (quark self-energy) is developed in Sec. IV, and the results are presented and discussed in Sec. V.

II. REVIEW OF THE MODEL

In the interest of completeness we give a brief review of the methods of I (Ref. 10), mentioning the few novel features which emerge in the two-nucleon problem. The reader is referred to I for a more complete discussion.

The energy of the bag is computed variationally in the static-cavity approximation using a Lagrange constraint to fix the expectation value of a collective variable. The variational expression is

$$\langle H_F - c_0 \mathcal{O} \rangle + BV, \tag{2.1}$$

where H_F is the Hamiltonian for the fields for a given cavity shape; $\mathcal{O}$ is the operator defining the collective variable; V is the cavity volume and c_0 and B are constants. Minimization of (2.1) with respect to the cavity shape determines the shape itself, and as c_0 is varied, one obtains an expression for the energy

$$E = \langle H_F \rangle + BV \tag{2.2}$$

as a function of $\langle \mathcal{O} \rangle$. Only axially symmetric cavities with reflection symmetry about the equatorial plane are considered. The surface is defined by the three-parameter formula in cylindrical coordinates:

$$\rho^2 = n^2(1 - z^2/d^2)(1 + az^2/d^2). \tag{2.3}$$

Although this parameterization permits a wide variety of shapes, it does not permit fission with a sharply indented neck. Since the fissioning regime was in any event considered to be beyond the range of validity of the computation, we did not undertake an improvement of the parameterization (2.3). It is quite adequate for the short and intermediate range where the departure from sphericity is slight.

The separation of the quark triplets is described in terms of two orbitals, left and right (L and R), which are expressed as a linear combination of orthogonal orbitals, one symmetric and one antisymmetric (S and A) with respect to the replacement $z \to -z$, where the z axis is the deformation axis. Thus the spatial part of the fermion spinors is written as

$$\begin{aligned} q_L &= q_S - \sqrt{\mu}\, q_A, \\ q_R &= q_S + \sqrt{\mu}\, q_A, \end{aligned} \tag{2.4}$$

where μ varies in the interval $[0,1]$ for minimal to maximal orbital separation.

Two choices of constraint are considered here. One is a measure of the distance between the two orbitals. We have chosen the same measure as used in I, namely,

$$\delta = \frac{2\sqrt{\mu}\,(1+\mu)}{1+\mu^2} \int q_S^\dagger(\vec{x}) q_A(\vec{x}) z\, dV. \tag{2.5}$$

(There is no legitimate operator corresponding to δ, so it is treated as a c number.) The other is the quadrupole moment defined with respect to baryon number density, namely,

$$Q = n_S Q_S + n_A Q_A, \tag{2.6}$$

where n_S and n_A are the operators giving the quark occupation number in the symmetric and antisymmetric states and

$$\begin{aligned} Q_S &= \tfrac{1}{3} \int q_S^\dagger q_S (3z^2 - r^2) dV, \\ Q_A &= \tfrac{1}{3} \int q_A^\dagger q_A (3z^2 - r^2) dV. \end{aligned} \tag{2.7}$$

These are normalized so that when $\mu = 1$ (so that $n_S = n_A$) and the orbitals are well separated, $Q \approx \delta^2 \approx r_{12}^2$ where r_{12} is the two-nucleon separation. Whether more than one collective variable should be used and which one is the proper choice are questions which can be answered only in a dynamical study of the collective motion of the system.

The effective Hamiltonian giving the field energy to second order in the gluon-coupling constant g restricted to states with quarks is given by

$$\begin{aligned} H_F = &\int dV : q^\dagger(-i\alpha \cdot \nabla + \beta m) q : \\ &+ \int dV \{ \tfrac{1}{2}[(\vec{E}^a)^2 + (\vec{B}^a)^2] - \vec{J}^a \cdot \vec{A}^a \} + E_0(V), \end{aligned} \tag{2.8}$$

where in the static limit

$$\begin{aligned} &J_\mu^a = g : \bar{q} \lambda^a \gamma_\mu q :, \\ &\nabla \cdot \vec{E}^a = J^{0a}, \quad \nabla \times \vec{B}^a = \vec{J}^a \ \text{ in } V \\ &\hat{n} \cdot \vec{E}^a = 0, \quad \hat{n} \times \vec{B}^a = 0 \ \text{ on } S \end{aligned} \tag{2.9}$$

and $E_0(V)$ is the finite part of the zero-point energy of the fields. With only two orbitals under consideration the quark-field operator becomes

$$\begin{aligned} q(\vec{x}) = \sum_{c,f,m} [&q_{Scfm}(\vec{x}) b_{Scfm} e^{-i\omega_S t} \\ &+ q_{Acfm}(\vec{x}) b_{Acfm} e^{-i\omega_A t}], \end{aligned} \tag{2.10}$$

where the b's are annihilation operators for the quark-cavity eigenmodes in the absence of gluons and c, f, and m are color, flavor, and spin quantum numbers. The unperturbed-cavity eigenmodes are defined by the equations

$$(-i\alpha\cdot\nabla+\beta m)q_n(\vec{x})=\omega_n q_n(\vec{x}) \text{ in } V,$$
$$i\alpha\cdot\hat{n}q_n(\vec{x})=-\gamma_0 q_n(\vec{x}) \text{ on } S. \tag{2.11}$$

When the field is inserted into the effective Hamiltonian we obtain terms both bilinear and quadrilinear in the quark creation and annihilation operators, which are depicted graphically in Fig. 1. The Hamiltonian may be written as a sum of terms each involving a c number configuration-independent energy, and an operator which depends on color, spin, flavor, and orbital quantum numbers. Its expectation value on a particular quark configuration gives the field energy

$$\begin{aligned}E_F=&n_S\omega_S+n_A\omega_A+W_{MSz}C_{Sz}+W_{MS\perp}C_{S\perp})+(W_{MAz}C_{Az}+W_{MA\perp}C_{A\perp})+(W_{MSAz}C_{SAz}+W_{MSA\perp}C_{SA\perp}+W_{ED}C_D)\\&+[(W_{MX\perp}+W_{EX\perp})C_{X1d}+(W_{MXz}+W_{EXz})C_{Xzd}+(W_{EX}+W_{MX})C_{Xd}]\\&+[(W_{MX\perp}-W_{EX\perp})C_{X1O}+(W_{MXz}+W_{EXz})C_{XzO}+(W_{EX}+W_{MX})C_{XO}]+E_{self}+E_0.\end{aligned} \tag{2.12}$$

The eight terms (not counting the zero-point energy E_0) have been grouped in order so as to correspond to the eight types of diagrams in Fig. 1. The four self-energy diagrams are all grouped in E_{self}. The terms ω_S, ω_A, W_{MSz}, etc. are shape-dependent, configuration-independent energies and the coefficients n_S, n_A, C_{Sz}, $C_{S\perp}$, etc. are configuration-dependent numbers which we call the "configuration factors." The various energy contributions appearing in (2.12) are determined by solving the Dirac and Maxwell equations variationally according to procedures described in I. We give a brief account of the steps leading from (2.8) to (2.12):

The terms denoted by W represent contributions from the gluon fields, of which there are three types corresponding to the three types of currents: two "diagonal" currents S-S and A-A, and one transition current S-A. Consider the S-S fields. The magnetic field operator can be written in a two-component basis for the spin as

$$\vec{B}^a_{SS}=\sum_{i,c,c',f,m,m'}\vec{B}_{SSi}b^\dagger_{Sc'fm'}\sigma^i_{m'm}\lambda^a_{c'c}b_{Scfm}, \tag{2.13}$$

where the index i on the c-number fields refers to the spinor basis, not the Euclidean basis of the field. When the field operator is inserted into the Hamiltonian and integrated over the volume of the cavity, some simplification occurs due to the azimuthal symmetry of the fields and the cavity with the result

$$\begin{aligned}\tfrac{1}{2}\int\vec{B}^a_{SS}\cdot\vec{B}^a_{SS}dV-\int\vec{J}^a_{SS}\cdot\vec{A}^a_{SS}dV&=-\tfrac{1}{2}\int\vec{B}^a_{SS}\cdot\vec{B}^a_{SS}dV\\&=W_{MSz}b^\dagger_S\sigma^3\lambda^a b_S b^\dagger_S\sigma^3\lambda^a b_S\\&\quad+W_{MS\perp}b^\dagger_S\vec{\sigma}^\perp\lambda^a b_S\cdot b^\dagger_S\vec{\sigma}^\perp\lambda^a b_S,\end{aligned} \tag{2.14}$$

where we have suppressed the spin, flavor, and color labels and used the notation

$$\vec{\sigma}^\perp=\sigma^1\hat{e}_1+\sigma^2\hat{e}_2. \tag{2.15}$$

The commutator resulting from the ordering of (2.14) contributes to the self-energy. The normal ordered expression represents the exchange of a gluon [diagram (c) of Fig. 1], and involves a possible interchange of spins and colors between the quarks. The other quantities in (2.12) are defined in a similar fashion:

$$\begin{aligned}-\tfrac{1}{2}\int(\vec{B}^a_{AA})^2dV&=W_{MAz}(b^\dagger_A\sigma^3\lambda^a b_A)^2+W_{MA\perp}(b^\dagger_A\vec{\sigma}^\perp\lambda^a b_A)^2,\\-\tfrac{1}{2}\int\vec{B}^a_{SS}\cdot\vec{B}^a_{AA}dV&=W_{MSAz}(b^\dagger_A\sigma^3\lambda^a b_A)(b^\dagger_S\sigma^3\lambda^a b_S)\\&\quad+W_{MSA\perp}(b^\dagger_A\vec{\sigma}^\perp\lambda^a b_A)\cdot(b^\dagger_S\vec{\sigma}^\perp\lambda^a b_S),\\-\tfrac{1}{2}\int|\vec{B}^a_{SA}|^2dV&=W_{MXz}(b^\dagger_A\sigma^3\lambda^a b_S)(b^\dagger_S\sigma^3\lambda^a b_A)\\&\quad+W_{MX\perp}(b^\dagger_A\vec{\sigma}^\perp\lambda^a b_S)\cdot(b^\dagger_S\vec{\sigma}^\perp\lambda^a b_A),\\\tfrac{1}{2}\int(\vec{E}^a_{SS}+\vec{E}^a_{AA})^2dV&=-\tfrac{1}{2}\int(\vec{E}_S-\vec{E}_A)^2dV(b^\dagger_S\lambda^a b_S)\\&\quad\times(b^\dagger_A\lambda^a b_A)\\&=-W_{ED}b^\dagger_S\lambda^a b_S b^\dagger_A\lambda^a b_A,\\\tfrac{1}{2}\int|\vec{E}^a_{SA}|^2dV&=W_{EXz}(b^\dagger_A\sigma^3\lambda^a b_S)(b^\dagger_S\sigma^3\lambda^a b_A)\\&\quad+W_{EX\perp}(b^\dagger_A\vec{\sigma}^\perp\lambda^a b_S)(b^\dagger_S\vec{\sigma}^\perp\lambda^a b_A)\\&\quad+W_{EX}(b^\dagger_A\lambda^a b_S)(b^\dagger_S\lambda^a b_A).\end{aligned} \tag{2.16}$$

All of these terms enter in the effective Hamiltonian (2.8). The configuration factors in (2.12) arise from taking the expectation value of the various operators (2.16) on the state defined in Sec. III below. They are

$$n_S = \langle b_S^\dagger b_S \rangle, \quad n_A = \langle b_A^\dagger b_A \rangle$$
$$C_{Sz} = \langle : b_S^\dagger \sigma^3 \lambda^a b_S b_S^\dagger \sigma^3 \lambda^a b_S : \rangle,$$
$$C_{S\perp} = \langle : b_S^\dagger \vec{\sigma}^\perp \lambda^a b_S b_S^\dagger \vec{\sigma}^\perp \lambda^a b_S : \rangle,$$
$$C_{Az} = \langle : b_A^\dagger \sigma^3 \lambda^a b_A b_A^\dagger \sigma^3 \lambda^a b_A : \rangle,$$
$$C_{A\perp} = \langle : b_A^\dagger \vec{\sigma}^\perp \lambda^a b_A b_A^\dagger \vec{\sigma}^\perp \lambda^a b_A : \rangle,$$
$$C_{SAz} = 2\langle : b_A^\dagger \sigma^3 \lambda^a b_A b_S^\dagger \sigma^3 \lambda^a b_S : \rangle,$$
$$C_{SA\perp} = 2\langle : b_A^\dagger \vec{\sigma}^\perp \lambda^a b_A \cdot b_S^\dagger \vec{\sigma}^\perp \lambda^a b_S : \rangle, \qquad (2.17)$$
$$C_{Xzd} = 2\langle : b_A^\dagger \sigma^3 \lambda^a b_S b_S^\dagger \sigma^3 \lambda^a b_A : \rangle,$$
$$C_{X1d} = 2\langle : b_A^\dagger \vec{\sigma}^\perp \lambda^a b_S \cdot b_S^\dagger \vec{\sigma}^\perp \lambda^a b_A : \rangle,$$
$$C_{Xd} = 2\langle : b_A^\dagger \lambda^a b_S b_S^\dagger \lambda^a b_A : \rangle,$$
$$C_{Xz0} = 2\langle : b_A^\dagger \sigma^3 \lambda^a b_S b_A^\dagger \sigma^3 \lambda^a b_S : \rangle,$$
$$C_{X10} = 2\langle : b_A^\dagger \vec{\sigma}^\perp \lambda^a b_S b_A^\dagger \vec{\sigma}^\perp \lambda^a b_S : \rangle,$$
$$C_{X0} = 2\langle : b_A^\dagger \lambda^a b_S b_A^\dagger \lambda^a b_S : \rangle,$$
$$C_D = -\langle : b_S^\dagger \lambda^a b_S b_A^\dagger \lambda^a b_A : \rangle.$$

The self-energy contribution from the S and A orbitals alone is given by

$$E_{self} = (W_{MSz} n_{Sz}^c + W_{MS\perp} n_{S\perp}^c) + (W_{MAz} n_{Az}^c + W_{MA\perp} n_{A\perp}^c) + (W_{MXz} + W_{EXz})(n_{Az}^c + n_{Sz}^c) + (W_{MX\perp} + W_{EX\perp})(n_{A\perp}^c + n_{S\perp}^c) + (W_{EX} + W_{MX})(n_A^c + n_S^c), \qquad (2.18)$$

where the first two terms grouped in parenthesis are represented by the S-S-S and A-A-A "diagonal" graphs in Fig. 1(h) and the remaining terms collect contributions from the off-diagonal graphs S-A-S and A-S-A. In writing (2.12) and (2.18) we have made use of the color-singlet property of the state which provides that the electric part of the graphs Figs. 1(c), 1(d), and 1(e) and the electric parts of the diagonal self-energy graphs Fig. 1(h) combine to give the term $W_{ED}C_D$ in (2.12) (see the discussion in the Appendix). The configuration factors in (2.18) are defined by

$$n_{Sz}^c = \langle b_S^\dagger (\lambda^a \sigma^3)^2 b_S \rangle, \quad n_{S\perp}^c = \langle b_S^\dagger (\lambda^a \vec{\sigma}^\perp)^2 b_S \rangle$$
$$n_{Az}^c = \langle b_A^\dagger (\lambda^a \sigma^3)^2 b_A \rangle, \quad n_{A\perp}^c = \langle b_A^\dagger (\lambda^a \vec{\sigma}^\perp)^2 b_A \rangle \qquad (2.19)$$
$$n_S^c = \langle b_S^\dagger (\lambda^a)^2 b_S \rangle, \quad n_A^c = \langle b_A^\dagger (\lambda^a)^2 b_A \rangle.$$

These are all simply proportional to the respective occupation numbers n_S and n_A. With our normalization for the matrices λ^a,

$$n_{Sz}^c = \tfrac{1}{2} n_{S\perp}^c = n_S^c = \tfrac{16}{3} n_S,$$
$$n_{Az}^c = \tfrac{1}{2} n_{A\perp}^c = n_A^c = \tfrac{16}{3} n_A. \qquad (2.20)$$

The expression for the self-energy actually used in the computation (4.5), (4.6) differs from (2.18), as discussed in Sec. IV.

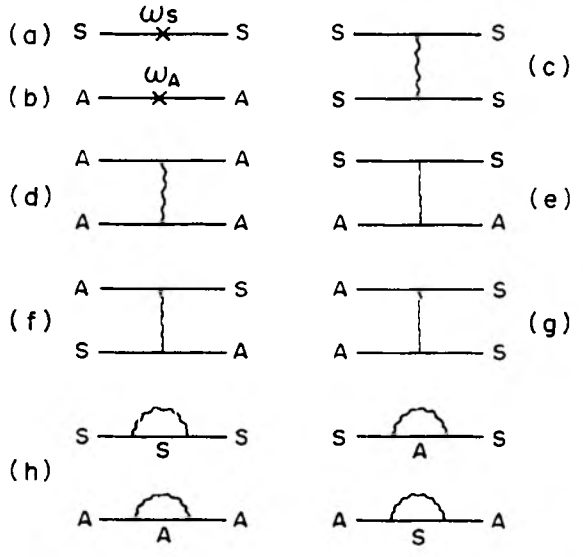

FIG. 1. Diagrams representing terms in the effective Hamiltonian.

III. SIX-QUARK-CONFIGURATION INTERNAL-SYMMETRY COEFFICIENTS

In Sec. II we presented an effective Hamiltonian for the state containing only quarks. We now proceed to define the state upon which its expectation value is to be evaluated. It will then be possible to evaluate explicitly the configuration factors (2.17).

We shall consider a color-singlet configuration of six nonstrange quarks with a definite total spin S and isospin I. If all quarks are found in the same spatial orbital, then the values I, S, and m_S specify the state uniquely. If we use the notation (r,y,b) for the quark colors, $(\uparrow,\downarrow)$ for the quark-spin projections, and (u,d) for the quark flavors, then the completely antisymmetrized wave function for $I=0$, $S=1$, $|m_S|=1$ is given by the antisymmetric part of a direct product of Young tableaux[11] as

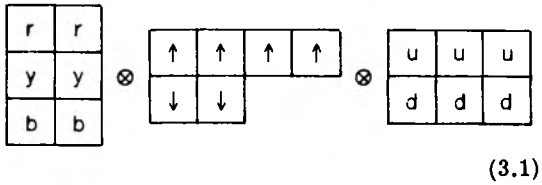

(3.1)

We want to consider the separation of the quarks into two spatial orbitals labeled L and R, each containing three quarks in a color-singlet state. (A separation into noncolor-singlet states would be energetically unfavorable because of the strongly attractive color-electrostatic force.) There are two possibilities for nonstrange quarks. Either the separation results in two nucleons or in two

$\Delta(1236)$ resonances. For a static calculation the state symmetric under the interchange of left and right spatial coordinates is appropriate, since it is convenient for generating the even partial waves in the two-baryon channel. For the spatial part of the wave function there are two Young tableaux with this property, namely,

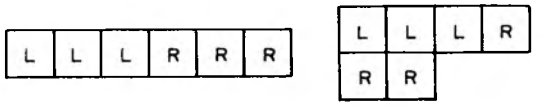

(3.2)

The first tableau is the only one which survives in the limit that all quarks appear in the same orbital, i.e., when $L \to R$. In general, however, both spatial configurations may contribute. This arbitrariness in the choice of spatial wave function is related to the arbitrariness in choosing a separation resulting in two nucleons or two Δ's

For present purposes we consider only the separation into two nucleons, thereby specifying the state uniquely. Of course the resulting configuration will necessarily overlap with the two-Δ configuration as long as the L and R orbitals are not orthogonal. Since we do not attempt to diagonalize the Hamiltonian on the two-baryon basis, we cannot discuss subtler effects caused by the interaction of these two channels, such as the question of how much $\Delta\Delta$ component there is in the deuteron. This question can be answered by a small extension of the present calculation.

The quark triplet with the quantum numbers of the proton and $m_s = \frac{1}{2}$ is created by the linear combination of quark-creation operators (in obvious notation)

$$\begin{aligned}(18)^{1/2} p^\dagger(\uparrow) = {} & 2u_r^\dagger(\uparrow)u_y^\dagger(\uparrow)d_b^\dagger(\uparrow) + 2u_r^\dagger(\uparrow)d_y^\dagger(\uparrow)u_b^\dagger(\uparrow) \\ & + 2d_r^\dagger(\uparrow)u_y^\dagger(\uparrow)u_b^\dagger(\uparrow) - u_r^\dagger(\uparrow)u_y^\dagger(\uparrow)d_b^\dagger(\uparrow) \\ & - u_r^\dagger(\uparrow)d_y^\dagger(\uparrow)u_b^\dagger(\uparrow) - d_r^\dagger(\uparrow)u_y^\dagger(\uparrow)u_b^\dagger(\uparrow) \\ & - u_r^\dagger(\uparrow)u_y^\dagger(\uparrow)d_b^\dagger(\uparrow) - u_r^\dagger(\uparrow)d_y^\dagger(\uparrow)u_b^\dagger(\uparrow) \\ & - d_r^\dagger(\uparrow)u_y^\dagger(\uparrow)u_b^\dagger(\uparrow).\end{aligned} \tag{3.3}$$

We have written $u_r(\uparrow)$ in place of $b_{ur\uparrow}$, etc. for ease in reading. The corresponding expression for the neutron is obtained by replacing $u \to d$ and $d \to -u$. If we label the spatial orbitals by L and R, the six-quark configuration with quantum numbers $I=0$, $S=1$, $|m_S|=1$, which we study in the present work, is given by the unnormalized expres-

TABLE I. Configuration-dependent coefficients for the six-quark system with $I=0$, $S=1$, $|m_S|=1$ as a function of the configuration-mixing parameter μ, defined by (3.6) in the text. The labels over the column headings refer to the relevant graph in Fig. 1.

	a	b	c		d		cde
μ	n_S	n_A	C_{Sz}	$C_{S\perp}$	C_{Az}	$C_{A\perp}$	C_D
0.0	6.00	0.00	8.53	−13.87	0.00	0.00	0.00
0.1	5.76	0.24	8.04	−12.56	0.16	0.33	1.06
0.2	5.25	0.74	7.03	−9.90	0.50	0.92	3.19
0.3	4.77	1.23	6.07	−7.43	0.87	1.30	5.06
0.4	4.37	1.63	5.31	−5.55	1.23	1.40	6.35
0.5	4.05	1.95	4.71	−4.16	1.56	1.27	7.17
0.6	3.78	2.22	4.24	−3.10	1.88	0.99	7.69
0.7	3.55	2.44	3.84	−2.27	2.18	0.64	8.00
0.8	3.35	2.65	3.51	−1.60	2.46	0.24	8.18
0.9	3.16	2.84	3.22	−1.05	2.72	−0.18	8.27
1.0	3.00	3.00	2.96	−0.59	2.96	−0.59	8.30

	e		f		g		
μ	C_{SAz}	$C_{SA\perp}$	$C_{X\perp d}$	C_{Xzd}	C_{Xd}	$C_{x\perp 0}$	C_{Xz0}	C_{X0}
0.0	0.00	0.00	0.00	0.00	0.00	0.00	0.00	0.00
0.1	0.60	2.88	−0.15	0.76	−1.97	10.33	2.33	−5.94
0.2	1.82	8.66	−0.46	2.28	−5.92	16.71	3.73	−10.03
0.3	2.90	13.74	−0.72	3.61	−9.40	19.69	4.34	−12.44
0.4	3.62	17.24	−0.91	4.54	−11.79	21.02	4.57	−13.93
0.5	4.10	19.48	−1.02	5.12	−13.32	21.69	4.66	−14.94
0.6	4.40	20.86	−1.10	5.49	−14.28	22.06	4.70	−15.63
0.7	4.58	21.72	−1.14	5.72	−14.86	22.30	4.72	−16.11
0.8	4.68	22.20	−1.17	5.84	−15.19	22.43	4.73	−16.40
0.9	4.72	22.44	−1.18	5.91	−15.36	22.50	4.74	−16.55
1.0	4.74	22.52	−1.19	5.93	−15.41	22.52	4.74	−16.59

sion

$$D^{\dagger}(+1)=p_R^{\dagger}(\uparrow)n_L^{\dagger}(\uparrow)+p_L^{\dagger}(\uparrow)n_R^{\dagger}(\uparrow). \tag{3.4}$$

The use of the algebra of creation operators simplifies the notation for the antisymmetrization of the state.

To define the contribution to the Hamiltonian it is useful to express the left and right orbitals in terms of the orthogonal symmetric (S) and antisymmetric (A) orbitals introduced in Sec. II. Thus, introducing a subscript for the spatial orbital, we have

$$\begin{aligned} u_{rL}^{\dagger}(\uparrow)&=u_{rS}^{\dagger}(\uparrow)-\sqrt{\mu}\,u_{rA}^{\dagger}(\uparrow),\\ u_{rR}^{\dagger}(\uparrow)&=u_{rS}^{\dagger}(\uparrow)+\sqrt{\mu}\,u_{rA}^{\dagger}(\uparrow), \end{aligned} \tag{3.5}$$

and similarly for all other operators. The resulting configuration, symmetrized under $L \rightleftharpoons R$ consists of a linear combination of the orbital occupations S^6, S^4A^2, S^2A^4, and A^6, with weights determined uniquely by μ and the internal symmetry quantum numbers. As μ varies on the interval $[0,1]$ a definite path in configuration space has been chosen. Since the nucleons are the lightest of the baryons, we suspect that path is the one which gives the best estimate of the ground-state energy.

Having defined the state, what remains is to compute the expectation value on this state of the various operators in the effective Hamiltonian (2.8) both bilinear and quadrilinear in the creation and annihilation operators for the quarks. The resulting expectation values give the configuration factors denoted by n_S, n_A, and C in the expression for the field energy of the cavity (2.11). As far as we know, there is no simple and straightforward procedure for finding all these quantities, although individual coefficients and combinations of coefficients can be found. The source of this difficulty lies chiefly with the introduction of a spatial degree of freedom with two permutation symmetries (3.2). We have accordingly made use of a high-speed computer to calculate these matrix elements essentially by brute force. The method is described in the Appendix.

We obtain the following result for the state with $I=0$, $S=1$, $|m_S|=1$:

$$\begin{aligned} &N=5+67(\mu^2+\mu^4)+5\mu^6\ ,\\ &n_S=(30+268\mu^2+134\mu^4)/N\ ,\quad n_A=6-n_S=(30\mu^6+268\mu^4+134\mu^2)/N\ ,\\ &C_{Sz}=(128+896\mu^2+256\mu^4)/3N\ ,\quad C_{S\perp}=(-208-608\mu^2+560\mu^4)/3N\ ,\\ &C_{Az}=(128\mu^6+896\mu^4+256\mu^2)/3N\ ,\quad C_{A\perp}=(-208\mu^6-608\mu^4+560\mu^2)/3N\ ,\\ &C_{Xz0}=2[192(\mu+\mu^5)+640\mu^3]/3N\ ,\quad C_{X\perp 0}=2[848(\mu+\mu^5)+3168\mu^3]/3N\ ,\\ &C_{X0}=-2[480(\mu+\mu^5)+2624\mu^3]/3N\ ,\quad C_{Xzd}=2\times 640(\mu^2+\mu^4)/3N\ ,\\ &C_{X\perp d}=-2\times 128(\mu^2+\mu^4)/3N\ ,\quad C_{Xd}=-2\times 1664(\mu^2+\mu^4)/3N\ ,\\ &C_{SAz}=2\times 512(\mu^2+\mu^4)/3N\ ,\quad C_{SA\perp}=2\times 2432(\mu^2+\mu^4)/3N\ ,\\ &C_D=1792(\mu^2+\mu^4)/3N\ . \end{aligned} \tag{3.6}$$

These factors are listed for a few values of μ in Table I.

IV. QUARK SELF-ENERGY

We now have available essentially all of the terms required to evaluate the field-energy of the cavity (2.12): the configuration factors given by (3.6) and the configuration-independent fermion energies ω_S and ω_A and the gluon-field energies denoted by W, computed according to the variational procedure given in I. The self-energy contribution $E_{\rm self}$ requires special treatment, which we describe here. The same treatment was adopted in I.

The complete quark self-energy to second-order in the color coupling constant is evaluated by summing diagrams of the type [Fig. 1(h)] for all possible intermediate states. The quark self-energy contributions perform three important functions in the bag:

(i) They provide the color-electric field component needed for the color-electric field to satisfy the linear boundary condition. This component arises from the diagram in which the fermion orbital remains unchanged in the intermediate state.

(ii) For massive fermions they generate an infinite mass renormalization. This infinite term arises from the short-distance free-field singularity in the fermion and gluon cavity propagators. (For massless quarks this infinite term is absent.)

(iii) They produce a finite-cavity Lamb shift which is orbital, mass, and shape dependent.

Previous phenomenological work in the static-

cavity approximation[7] has made use of only the first two of these functions for computations with spherical cavities. In the work of Ref. 7 the finite part of the zero-point energy of the fields in a sphere of radius R is introduced with a term

$$E_0 = -Z_0/R \ , \tag{4.1}$$

where Z_0 is determined phenomenologically by adjusting the masses of the states. For massless quarks, the cavity Lamb shift has the same form. Thus, one might say in partial defense of the procedure of Ref. 7, that the Lamb shift has already been absorbed in the determination of Z_0; what was called the zero-point energy is, in fact, a combination of zero-point energy and Lamb shift:

$$-Z_0/R = -Z_0'/R + \sum_i n_i \delta\omega_i \ , \tag{4.2}$$

where n_i is the quark-occupation number of orbital i, $\delta\omega_i$ is the corresponding Lamb shift, and Z_0 is the true zero-point energy parameter for the sphere. Thus the effective value of Z_0 could well be different for mesons and nucleons which have different quark numbers. Although choosing different values for these two species might well improve the mass calculations, there is no compelling reason to do so, given the nature of other approximations of the model. A phenomenological determination of $\delta\omega_i$ is not called for at present.

To compute the finite Lamb shift theoretically involves a summation over all intermediate fermion and gluon states, a task which is apparently not possible in closed form for the sphere, and all the more hopeless for cavities of general shape. However, some ingenuity[12] may provide an indication of the shape dependence of these terms.

We have explored the possibility of evaluating the spherical-cavity Lamb shift for the two orbitals of present interest by summing over a few lowest-energy fermion intermediate states. The series does not appear to converge very rapidly in the covariant gauge although it was felt that in this gauge convergence would be more rapid than in others.[13] However, an interesting qualitative feature emerges which is relevant to the two-orbital treatment of quark separation. The substantial negative magnetic-dipole terms in the diagonal transition $S_{1/2}$-$S_{1/2}$-$S_{1/2}$ are nearly cancelled by the electric dipole and magnetic-quadrupole terms in $S_{1/2}$-$P_{3/2}$-$S_{1/2}$ when all permissible values $|m_j| = \frac{1}{2}$ and $\frac{3}{2}$ occur in the intermediate state. The corresponding statement is also true for the $P_{3/2}$ level. Thus if only these two orbitals appear, the resulting cavity Lamb shift is less than 10% of the magnitude of the individual terms. (Of course higher contributions may well alter this result.) Thus for want of any better procedure short of an exhaustive study of this problem, in what follows, we shall restrict our attention to these two orbitals and assume this cancellation takes place in the sphere. We may then accept the parameterization of the zero-point energy of Ref. 7 (and the other parameters) at face values and put

$$\begin{aligned} \delta\omega_S(\text{sphere}) &= 0 \ , \\ \delta\omega_A(\text{sphere}) &= 0 \ , \end{aligned} \tag{4.3}$$

so that Z_0 is the same for both mesons and baryons.

Having established a procedure for treating a spherical cavity, let us consider other shapes. Obviously, if the cavity should divide into two spheres, for consistency, the descriptions should correspond in each sphere to what we have already established for one. Here an interesting and important constraint on the handling of self-energies emerges. When the cavity divides into two spheres, the orbitals S and A become degenerate linear combinations of S-type orbitals for the left and right spheres. Let us call these individual orbitals S_L and S_R. Obviously, the electric-monopole terms in the self-energy diagrams S_L-S_L-S_L and S_R-S_R-S_R are needed in order to satisfy the linear-boundary condition for the color-electric fields in the individual spheres. If we reexpress these contributions in terms of the orbitals S and A we discover that we are actually computing the electric part of the off-diagonal self-energy terms S-A-S and A-S-A together with the diagonal contributions. Thus, for the fissioning cavities, the electric part of the S-A-S and A-S-A self-energy terms are *essential* in providing for the confinement of color-electric flux. Notice also, that the magnetic terms in the diagonal contribution S_L-S_L-S_L and S_R-S_R-S_R must now, according to our prescription for the sphere, be cancelled by higher terms of the type S_L-A_L-S_L, etc. These new intermediate states correspond in the language of the single cavity to still higher orbitals with more modes which we have not considered.

Further evidence for the physical importance of the electric terms in S-A-S and A-S-A may be found by considering the separation of a quark and antiquark in a long cavity as discussed in I. In this configuration one might expect that for large separations of the quarks, the classical result would be obtained—namely, that the field energy is that of two opposite classical charges separated by an appropriate distance, with field lines confined to the cavity. If the charge distribution is described in terms of the orbitals S and A, a careful exercise in bookkeeping reveals that only half of the required field energy arises from gluon-exchange diagrams.[10] The other half comes from the self-

energy terms—in particular, the electric terms in S-A-S and A-S-A.

To summarize, therefore, in the notation of (2.18) we must have in the two-bag limit

$$\delta\omega_S = \delta\omega_A - \tfrac{16}{3} W_{EX} \ . \tag{4.4}$$

Having established the two limits (4.3) and (4.4), we seek a smooth interpolation between them. Since we have not carried out the full quantitative analysis of the self-energy series, we make what appears to be the most straightforward interpolation based upon a truncation of the series at the lowest two orbitals, regarding these orbitals as essentially degenerate. We shall find that with only minor modifications the two-orbital expression (2.18) can be used for the interpolation. The modifications which we require involve enforcing (4.3) explicitly, and arranging for the spherical symmetry of the $S_{1/2}$ Lamb shift. These are now discussed.

Our analysis of the gluon fields provides contributions from the four transitions S-S-S, S-A-S, A-A-A, and A-S-A in which the intermediate quark orbital has a magnetic quantum number $|m_j| = \frac{1}{2}$ and in which the states S and A are taken to be degenerate. In the sphere, the state A is indentified with $P_{3/2}$ and there are two other states with $|m_j| = \frac{3}{2}$ with which it is exactly degenerate. As the sphere is distorted into a prolate ellipsoid the magnetic terms in S-S-S and A-A-A fall off. This can be seen in Fig. 2, curve (a) where the quantity $-(W_{MS\parallel} + 2W_{MS\perp})/\alpha$ is displayed for cavities of ellipsoidal shape with unit equatorial radius and a range of values of the polar radius d. This quantity is proportional to the negative of the contribution from the magnetic terms in S-S-S. The curve (b) displays $-(W_{MA\parallel} + 2W_{MA\perp})/\alpha$ corresponding to the negative of the magnetic terms in A-A-A. The spin-independent $E_{1,0}$ electric terms in S-A-S and A-S-A grow quite rapidly, because they represent the field produced by the separation of two opposite charges towards the poles of the ellipsoid. This term is displayed in the form $(W_{EX} + W_{MX})/\alpha$ as curve (c) of Fig. 2. The $E_{1,1}$ field produced by the transition S-$A_{3/2}$-S, i.e., to the lowest antisymmetric state with $|m_j| = \frac{3}{2}$, is not computed. However, we can get some feeling for the qualitative shape dependence of its energy by resorting to the following argument: The form of the transition charge density is that of two charges separating lengthwise (parallel to the deformation axis) along the ellipsoid. Thus the field energy should fall with increasing length for long cavities of fixed equatorial radius. For spherical shapes it can be shown that the total contribution from intermediate states of all magnetic quantum numbers should exert a spherically symmetric pressure for the $S_{1/2}$ level. The same is not true for the $P_{3/2}$ level, however. Thus the derivative of the level shift for the S orbital with respect to length should vanish for spherical shapes. Our estimate of the contribution from this term is shown for ellipsoidal cavities in Fig. 2(d) and the resulting total contribution Fig. 2(e) of Figs. 2(c) and 2(d) is seen to have minimum at the spherical shape $d = 1$.

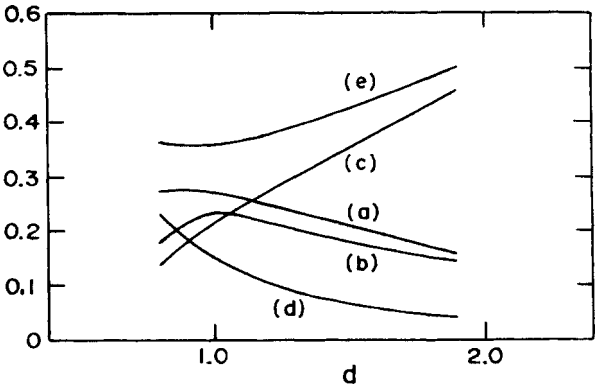

FIG. 2. Components of the self-energy evaluated in the approximation of degenerate orbital energies for cavities of ellipsoidal shape with unit equatorial radius and of polar radius d (see Sec. IV for details).

Since the self-energy contributions that we can compute and estimate already have nearly the desired qualitative behavior, we take them with small modification and write the self-energy (cavity Lamb shift) as follows:

$$\delta\omega_S = \tfrac{16}{3}[(W_{EX} + W_{MX}) + c_1 n/d^2 R_0 + (W_{MS\parallel} + 2W_{MS\perp}) x c_2], \tag{4.5a}$$

$$\delta\omega_A = \tfrac{16}{3}[(W_{EX} + W_{MX}) + (W_{MA\parallel} + 2W_{MA\perp}) x c_3], \tag{4.5b}$$

$$x = 1 - (1 - n/d)^2 . \tag{4.5c}$$

The terms W_{EX}, W_{MX}, etc. are defined in Sec. II. The level shift for the S orbital is comprised of three parts grouped in [4.5(a)]. The first term gives the positive, spin-independent contribution from the S-A-S transition and corresponds to the $E_{1,0}$ component in the sphere [Fig. 2(c)]. The second term estimates the contribution from the other terms, including those corresponding to the $E_{1,1}$ and $E_{1,-1}$ components in the sphere [Fig. 2(d)]. [We have omitted several small terms in (2.18).] The geometrical parameters n and d are defined in Sec. II. The parameter R_0 is the maximum value attained by ρ on the surface (2.3). The constant c_1 is adjusted so that δE_S is minimum for the sphere, as discussed above ($c_1 = 0.081$). The third term in [4.5(a)] represents the magnetic contribution from the diagonal S-S-S transition [Fig. 2(a)] with a coefficient x which suppresses this term as

fission takes place ($n/d \to 0$). The constant c_2 is adjusted so that the level shift vanishes exactly for the sphere ($c_2 = 1.34$). The level shift for the A orbital is constructed in such a way that it also vanishes for the sphere ($c_3 = 0.93$). Both constants, c_2 and c_3, are nearly equal to unity since the desired cancellation is nearly automatic. The net contribution to the field energy of the cavity is weighted by the occupation number. Thus

$$E_{self} = n_S \delta\omega_S + n_A \delta\omega_A , \tag{4.6}$$

together with (4.5) takes the place of (2.18).

We feel that this treatment of the level shift represents the most straightforward approach which provides an expression consistent with our qualitative expectations for the behavior of the self-energy and with the desire for a minimum of complication. Of all contributions explicitly incorporated into the model it is the most uncertain, and it offers the greatest theoretical challenge.

V. RESULTS AND DISCUSSION

Calculations were carried out following the same variational procedure as in I. For the color-coupling constant and bag-pressure constant we have used the values $\alpha_c = 0.54$ and $B^{1/4} = 145$ MeV, essentially the same as were used in Ref. 7. These and the constant normalizing the zero-point energy discussed in I give the correct masses of the nucleon and Δ, a matter of obvious importance to the present calculation.[14]

The present calculation refers to a six-quark system with total isospin zero, spin one, and spin projection one on the deformation axis. The result of minimizing the energy at a fixed value of the separation parameter δ (2.5) is presented in Fig. 3 (solid curve). The mass of two noninteracting nucleons has been subtracted to give the interaction energy shown. The interaction is repulsive for $\delta \lesssim 0.35$ fm and exhibits a "soft" repulsive core attaining a maximum repulsion of ~285 MeV at zero separation. The interaction is attractive at intermediate range $\delta \gtrsim 0.35$ fm, with maximal attraction appearing at $\delta = 0.8$ fm at ~ −180 MeV. The energy rises above that of two nucleons at $\delta \gtrsim 1.4$ fm—this last feature is believed to be an artifact of the cavity geometry (2.3) since it occurs for cavity volumes considerably larger than that of two nucleons.[15] (At $\delta = 1.4$, $BV \approx 600$ MeV compared with $BV \approx 470$ MeV for two nucleons.) The two-nucleon volume is reached at $\delta \approx 1$ fm when the cavity has a slightly nonspherical geometry. The one-pion exchange potential[16] for two pointlike nucleons separated by the distance δ is also plotted in Fig. 3 for comparison. It is striking that in the region $1 < \delta < 1.2$ fm both expressions for the interaction energy are more or less in agreement. Presumably this value of δ is the best choice for the change-over from the six-quark to the two-nucleon descriptions.

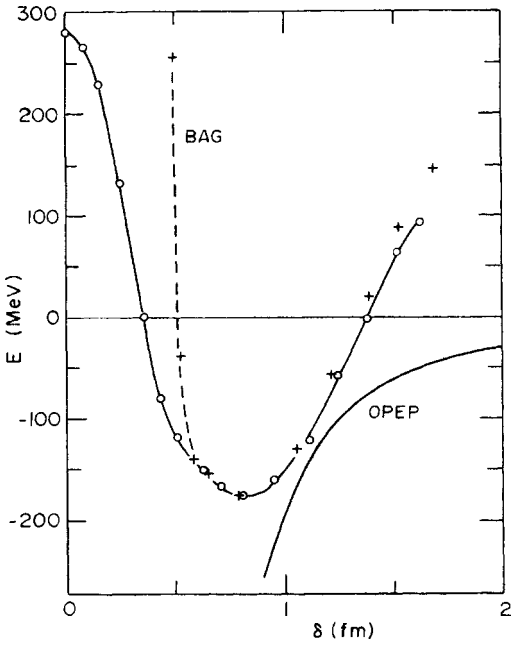

FIG. 3. Two-nucleon interaction energy (MeV) vs separation parameter δ (fm) for the six-quark system with $I = 0$, $S = 1$, $|m_s| = 1$ (solid line with circles), computed variationally at fixed separation. Shown for comparison are the one-pion-exchange potential (Ref. 16) (solid line) and the interaction energy computed variationally at fixed quadrupole moment (dashed line and plus signs).

The existence of a repulsive core in the single-orbital six-quark system has already been noted for spherical shapes.[7] It is due to a repulsive magnetic-gluon interaction (the same repulsive effect that makes the Δ more massive than the nucleon) in the configuration in which all quarks occupy the same spatial orbital. The repulsive core also depends critically on the presence of a negative zero-point energy as proposed in Ref. 7, since this term serves to lower the two-nucleon mass relative to the energy of the spherical, single-orbital six-quark system. The repulsion is still greater in isotriplet states.

The intermediate-range attraction obtained in the present calculation could not have been predicted without a quantitative calculation. Although the color-magnetic repulsion of the single-orbital system is expected to diminish, as separation into two orbitals takes place, this effect alone is not strong enough to result in attraction. Instead, an examination of the magnitudes of the various ener-

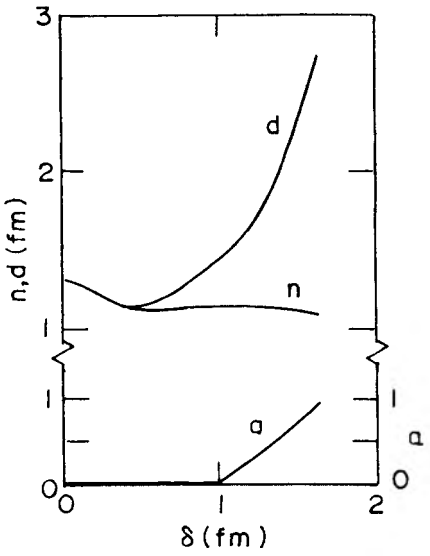

FIG. 4. Cavity geometrical parameters (2.3) vs the constrained separation parameter δ.

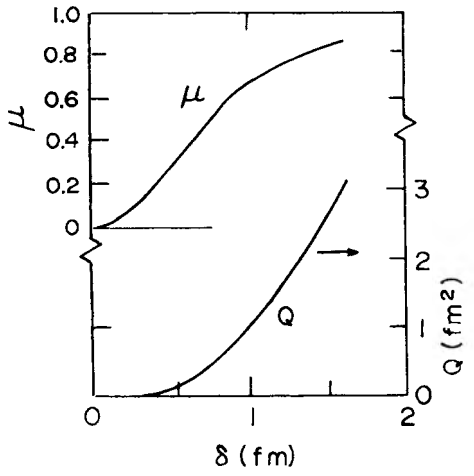

FIG. 5. Configuration-mixing parameter (μ) and baryonic quadrupole moment Q as a function of the constrained separation parameter.

gy contributions suggests that the main cause of the effect is a strong color-electrostatic attraction within the quark triplets (see below).

The quark triplets are quite well organized at $\delta = 1.2$ fm with the configuration-mixing parameter $\mu \approx 0.75$ corresponding to a 25% overlap in left and right orbitals. Thus the dominating factor in the long-range interaction appears to be the cavity geometry, as we have argued above, with quark interchange playing a secondary role.

We display the geometrical factors for the cavity shape in Fig. 4. The expression for the self-energy (4.5) has the tendency to make a negative (≈ -0.5) at zero separation. This effects lowers the overall repulsive maximum by about 30 MeV. Since it was judged to be an artifact of the approximation (4.5), and in any case within the error expected in the computation, we have for the sake of simplicity forced $a \geq 0$. (In obtaining spherical symmetry for the $S_{1/2}$-state Lamb shift, the a-dependence was not taken into account.) Thus for distances $\delta \lesssim 0.5$ fm the cavity shape remains spherical (to within 5% in the ratio of the major to minor radius) and shrinks in radius with increasing δ. A nonspherical shape appears only when the energy is close to minimum, after which the cavity becomes rapidly elongated. Fission occurs when $n \to 0$ and $a \to \infty$. For values of $a \leq 1$, the maximum cylindrical radius attained is given by n. The corresponding value for the nucleon is about 1 fm, only slightly less than that attained by the six-quark bag after reaching the energy minimum. It is interesting to note that the cavity semimajor axis d rises above the bag-nucleon diameter (2 fm) at $\delta = 1.2$ fm, and is consistent with our previous reasoning that with an improved cavity geometry, fission would occur near this point.

In Fig. 5 we show the configuration-mixing parameter as a function of the separation parameter. It is a measure of the degree of separation of the left and right orbitals. It is interesting that at the energy minimum it has already attained a value of 0.5 and rises rapidly to 1. Fission cannot take place until $\mu = 1$, since only then are the left and right clusters color singlets. Also shown in Fig. 5 is the baryonic quadrupole moment as a function of the constrained separation.

The baryon number density is shown in Figs. 6(a), 6(b), 6(c) for three choices of separation, and in Fig. 6(d) the density for two noninteracting spherical nucleons is shown for comparison. The development of concentrations of quarks in the two halves is well pronounced in Fig. 6(c).

The various contributions to the energy are analyzed in Figs. 7 and 8 and Table II. The total field energy (exclusive of the zero-point energy) and volume energy follow rather closely the total energy, with the volume energy (and therefore the volume) reaching a minimum at a smaller separation than the total field energy. The zero-point energy has a rather weak separation dependence but generally decreases. The several contributions to the field energy are shown in Fig. 8. The fermion kinetic energy actually rises steeply as the quark triplets are localized and the volume is reduced in passing from the repulsive core to the minimum.

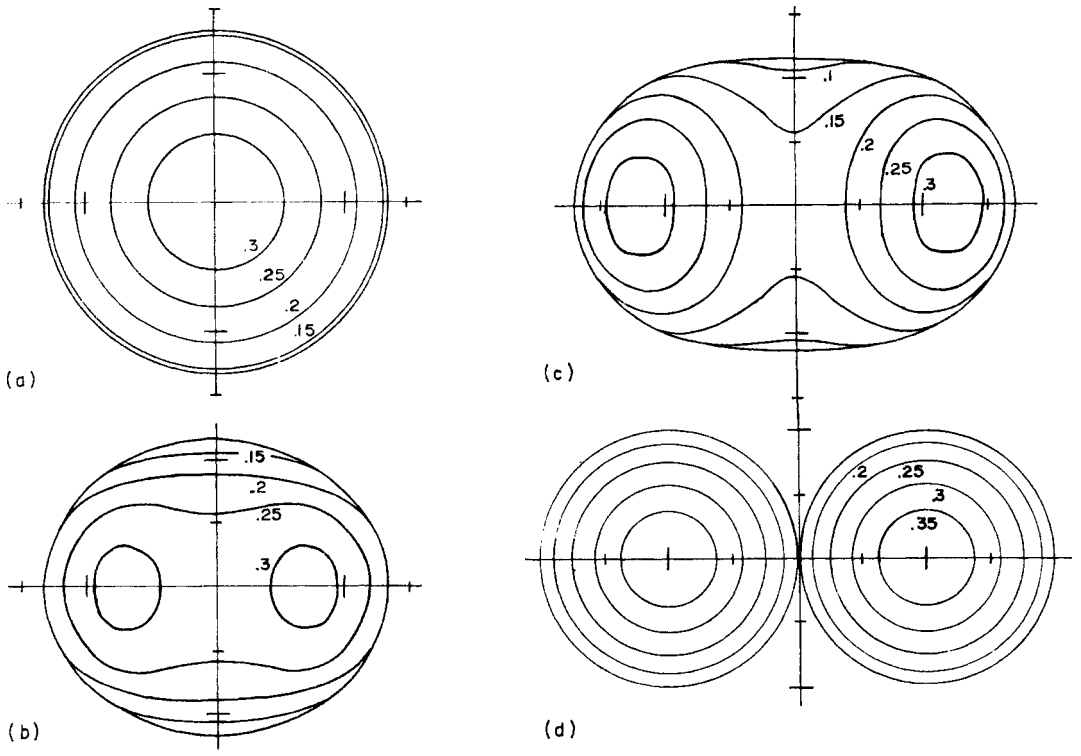

FIG. 6. Curves of equal baryon density (baryons/fm^3) in a full longitudinal cross section of the six-quark bag at various constrained separations: (a) $\delta = 0$; (b) $\delta = 0.8$ fm, minimum energy; (c) $\delta = 1.4$ fm; (d) Two noninteracting nucleons for comparison. Scale markings are in 0.5 fm.

The predominantly color-magnetic contributions from the diagrams (c, d, and e) in Fig. 1, so labeled in Fig. 8, show a mild decrease, turning negative, as they should for the nucleon configuration. The terms which drive the attraction are evidently the gluon-exchange diagrams of Figs. 1(f) and 1(g), shown in curves with the same labels in Fig. 1. The dominant contribution to these terms arises in turn from color-electric fields generated by the A-S transition. It is precisely the same terms which give rise to the strong attraction between quark and antiquark in I that produce the strong color-singlet condensation here. As a simple illustration of this condensation phenomenon, consider the elementary problem in quantum mechanics of two spherical infinite-potential wells barely connected and containing two electrons and two positrons. The ground-state orbital is nearly degenerate, consisting of one symmetric and one antisymmetric spatial orbital. From these one may construct left and right orbitals as in (2.4). All particles can be placed in the symmetric orbital, or a positron and an electron can be placed in the left orbital and the other pair in the right orbital. The latter configuration has a lower electrostatic energy because the attracting members are more strongly correlated. A similar effect occurs in a spherical cavity, but the lack of degeneracy in this case means that the increased electrostatic attraction must compete with an increased kinetic energy due to the localization of the particles. In the six-quark bag the color-electrostatic attraction is very strong and has no trouble in overcoming the increase in kinetic energy due to the localization of the quarks as can be seen in Fig. 8.

The self-energy contribution (right scale in Fig. 8) grows sharply as soon as the cavity elongates. It is zero for spherical shapes according to the prescription of Sec. III. Thus the shape of the curve of Fig. 3 up to separations of 0.5 fm is *unaffected* by the approximation (4.5). If we restrict our attention to purely spherical shapes with no self-energy included, an energy minimum occurs at about the same separation, but about 20 MeV higher. Varying the shape can only lower the result. Thus we have established an upper bound on the intermediate-range minimum at about −160 MeV in keeping with the assumption (4.3) that no net Lamb shift occurs in the sphere. This result could be changed, however, if it develops that ei-

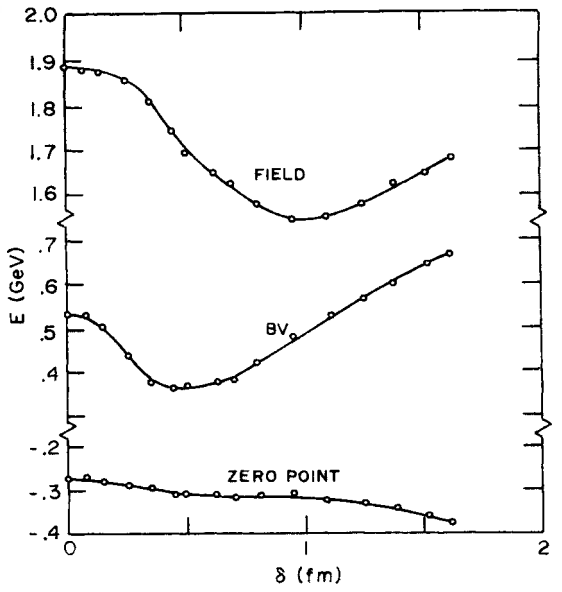

FIG. 7. Total field energy (excluding zero-point energy), volume energy, and zero-point energy of the six-quark bag as a function of constrained separation δ.

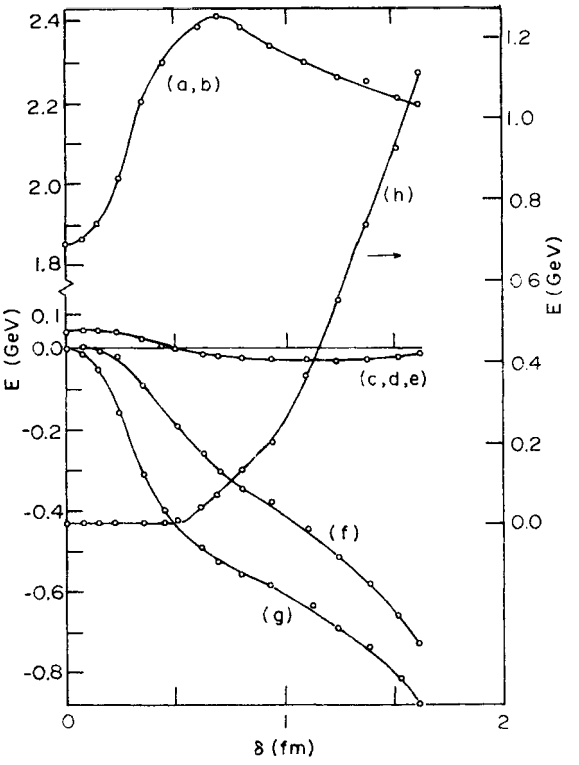

FIG. 8. Energy contributions corresponding to the graphs of Fig. 1 plotted vs constrained separation δ. The labeling is the same as in Fig. 1.

ther orbital is shifted, since it obviously depends upon a rather important compensation between the orbital kinetic energy and the electrostatic interaction energy. However, there is hope that the full Lamb shift can be evaluated more readily for spherical geometries; in that event this method of obtaining an upper bound may well prove to be useful. The behavior of the self-energy at $\delta \gtrsim 0.5$ fm has an important effect on the total energy: It is essential to include it if fission is to take place. At the point of fission $\mu \to 1$, and the self-energy contribution cancels the electrostatic contribution of graphs (f) and (g) of Fig. 1. To see to what extent the cancellation is taking place prior to fission in our treatment, we present in Fig. 9 the total of all gluon contributions to second order. The value for two nucleons is −310 MeV, or about 200 MeV above the values of Fig. 9 at the largest separations.

If we allow for a reasonable 30% error in the determination of the self-energy from the approximation (4.5) we see that there could be an error of 50–100 MeV in the result for the energy at $\delta \gtrsim 1$ fm but an error of $\lesssim$30 MeV for $\delta \lesssim 0.7$ fm. These errors are larger than the next largest expected contribution, namely, an error of approximately 10% in the variational determination of the gluon-exchange energies, due to the neglect of the S-A energy difference. (We do not attempt to estimate errors due to the choice of the model—the static-cavity approximation, the neglect of quark-antiquark pairs, the effect of higher-order gluon contributions, etc.)

When the same calculation is carried out at a fixed baryonic quadrupole moment (2.5) an interesting result appears and is shown in Fig. 10 and Table III. Because arbitrarily negative quadrupole moments may occur, a different aspect of the "short-range" interaction can be explored. In this case there appears to be an infinitely repulsive core (the computation was stopped when the curve reached about +1 GeV with no sign of a maximum). As the quadrupole moment is decreased from zero, the separation parameter (at constrained values of the quadrupole moment) begins decreasing very slowly (possibly to a limit) and the cavity develops an approximately oblate ellipsoidal shape. The larger negative values of the quadrupole moment are attained by a simple scaling-up of the bag dimensions. For oblate shapes there is a natural negative quadrupole moment. The volume increases accordingly and gives the large values for the energy.

It is interesting to replot the quadrupole-constraint curve as a function of the separation parameter. This is done in Fig. 3 (the plus signs and dashed line). When this curve is compared with what was obtained using only the separation param-

TABLE II. Energy contributions, baryonic quadrupole moment Q, and mixing parameter μ at various values of the constrained separation δ for the six-quark state $I=0$, $S=1$, $|m_S|=1$. All energies are in MeV. E_{quark} is the kinetic energy of the quarks, E_{cde}, E_{f}, E_{g}, E_{h}, the contributions of the graphs of the same label in Fig. 1, and E_0, the zero-point energy. The last line gives the corresponding parameters for two nucleons.

δ (fm)	Q (fm^2)	μ	E_{quark}	E_{cde}	E_{f}	E_{g}	E_{h}	BV	E_0	E_{tot}
0.00	0.00	0.000	1853	39	0	0	−5	537	−278	2147
0.08	0.00	0.007	1863	40	0	−15	−5	529	−279	2133
0.14	0.00	0.026	1902	40	−3	−56	−5	500	−285	2093
0.24	0.02	0.073	2013	36	−22	−160	−5	435	−298	2000
0.36	0.06	0.159	2203	21	−91	−318	−5	370	−314	1866
0.45	0.10	0.233	2297	5	−155	−402	−5	362	−317	1786
0.50	0.13	0.284	2330	−5	−191	−436	−4	370	−315	1750
0.62	0.28	0.373	2387	−17	−261	−497	34	377	−319	1704
0.70	0.43	0.434	2410	−21	−307	−535	78	384	−323	1686
0.81	0.61	0.516	2386	−26	−347	−565	130	420	−320	1679
0.95	0.87	0.651	2345	−27	−383	−582	190	478	−313	1708
1.11	1.27	0.721	2297	−27	−451	−636	367	527	−322	1756
1.25	1.76	0.760	2258	−32	−516	−687	553	570	−335	1810
1.38	2.22	0.824	2251	−30	−589	−754	744	596	−351	1865
1.53	2.75	0.850	2208	−22	−657	−810	929	644	−364	1929
1.62	3.14	0.872	2195	−16	−730	−881	1110	668	−379	1968
∞		1.000	2448	−312		0		466	−734	1868

eter as a constraint, we expect that the energy should be increased at a given value of δ when the quadrupole constraint is imposed in accordance with the variational principle. Indeed this result is obtained. But we also find a remarkable agreement between the two curves at large separation. Agreement should be exact at the overall minimum, since here no constraints are imposed. But the fact that this agreement persists to within 10–20 MeV at all separations larger than the minimum suggests that the baryonic quadrupole moment and separation parameter may be regarded as equivalent variables in this range. For separations $\delta \lesssim 0.5$ fm the variables depart drastically. A similar effect is seen when the points from the curve generated by constraining the separation are plotted as a function of quadrupole moment (see Fig. 10). The curves agree for $Q \gtrsim 0.1$ fm^2, but the separation constrained points rise to 280 MeV at zero quadrupole moment.

Which of the two collective variables to use (or whether both should be used) is a matter which can be answered only in a dynamical study. Essentially what is expected is that in a many-parameter description the variable which lies more nearly on the trajectory of "least resistance" as the system climbs out of the potential minimum is the best candidate for a single collective coordinate. Since we have not carried out the multiparameter calculation, we cannot draw any firm conclusions.

A number of future lines of research are suggested by these results:

(1) One is the investigation of other channels. With results for $I=0$, $S=1$, $M_S=0$, and the isotriplet channel it should be possible to isolate the spin-spin, tensor, and central components of the two-nucleon interaction.

(2) There is the interesting question of developing

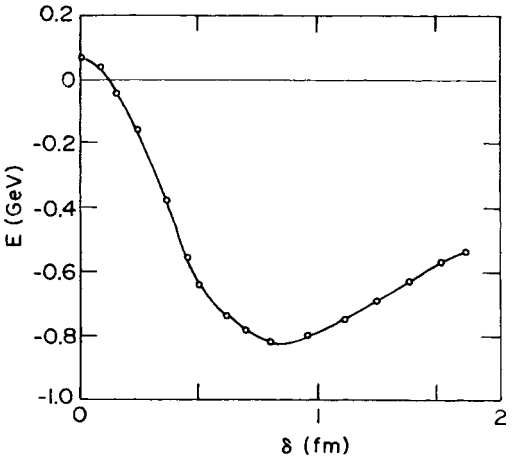

FIG. 9. The total contribution of gluon exchange and estimated self-energy to second order vs the constrained separation δ.

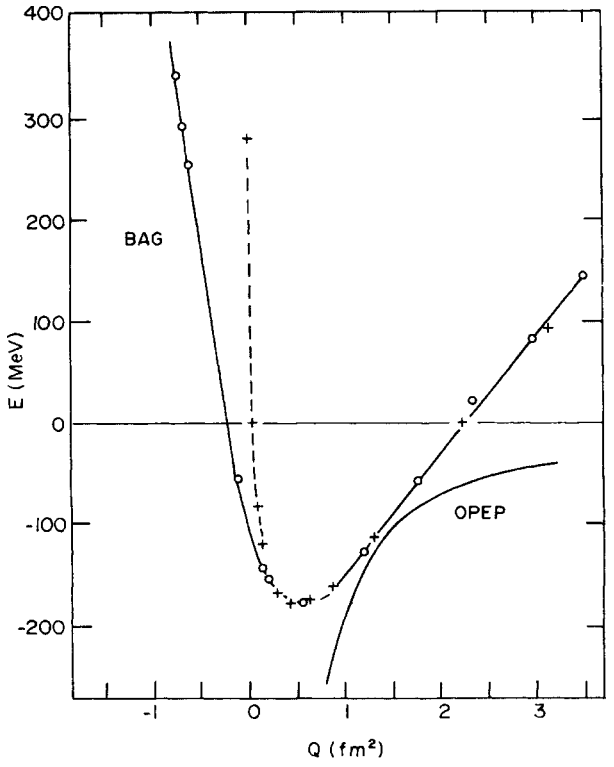

FIG. 10. Two-nucleon interaction energy vs the constrained baryonic quadrupole moment Q (fm^2) for the six-quark system with $I=0$, $S=1$, $|m_s|=1$ (solid line with circles). Shown for comparison are the one-pion-exchange potential (Ref. 16) (solid line) and points from Fig. 3 plotted as a function of Q (dashed line and plus signs).

TABLE III. Geometrical parameters and total energy of the six-quark system with $I=0$, $S=1$, $|m_S|=1$, computed at a fixed value of the baryonic quadrupole moment. Geometrical parameters are defined in Sec. II.

Q (fm^2)	δ (fm)	$E_{\rm tot}$ (MeV)	d (fm)	n (fm)	a
−0.72	0.48	2213	1.40	1.75	−0.3
−0.64	0.50	2162	1.36	1.70	−0.2
−0.60	0.49	2121	1.32	1.65	−0.2
−0.13	0.53	1828	1.21	1.34	−0.2
0.14	0.58	1724	1.19	1.19	−0.1
0.19	0.65	1714	1.20	1.20	−0.1
0.49	0.77	1686	1.28	1.17	0.0
1.21	1.05	1742	1.49	1.15	0.2
1.75	1.22	1812	1.68	1.20	0.2
2.32	1.39	1886	1.79	1.20	0.4
2.95	1.56	1951	1.91	1.19	0.6
3.54	1.69	2014	2.02	1.19	0.8

a dynamical description for the six-quark component of the deuteron at short range. From this the various static properties of the deuteron can be calculated.

(3) Adding the $\Delta\Delta$ component could help to resolve the question of its significance in the two-nucleon interaction.

(4) The deep-inelastic structure function for electron scattering from deuterons depends very sensitively upon the six-quark nature of the state[17] for values of the scaling variable in the range $1 \lesssim x < 2$. A better understanding of this component of the deuteron wave function may not help much in extracting information about the structure function of the neutron, but could be used to make a direct comparison between theory and experiment for the structure of the deuteron.

(5) The strong color-electrostatic condensation observed in the six-quark bag is undoubtedly of relevance to an understanding of the transition from high density to low density in neutron stars.

ACKNOWLEDGMENTS

Preliminary work was carried out at the Stanford Linear Accelerator Center and the Los Alamos Scientific Laboratory. The hospitality of the SLAC theory group and the LASL T-8 division is gratefully acknowledged. I would like to thank my present and past colleagues at the Center for Theoretical Physics, and in particular Alan Chodos, Bob Jaffe, Ken Johnson, Arthur Kerman, Jeffrey Mandula, Ernest Moniz, John Negele, and Charles Thorn for discussions which contributed to many of the ideas behind this work.

APPENDIX: COMPUTATION OF CONFIGURATION FACTORS

We describe here the computational procedure used to evaluate the expectation value of the configuration dependent operators (2.17) on the six-quark state defined in Sec. III. Since we were unable to find a simple analytical approach that gave all of the desired matrix elements, it was necessary to use a high speed computer. The results are consistent with a number of simple tests.

The method of computation was essentially by direct use of the anticommutator algebra of the fermion creation and annihilation operators; this is the most foolproof method. Computation was made more efficient through use of the following device: Products of spin and color generator matrices can be expressed in terms of permutation operators

$$\sigma_1^i \cdot \sigma_2^i = 2P_{12}^{\sigma} - 1 = \sigma_1^3 \sigma_2^3 \,, \qquad \lambda_1^a \lambda_2^a = 2P_{12}^{\lambda} - \tfrac{2}{3} \,. \tag{A1}$$

In each case the product of matrices acts on a direct product basis of spinors and the permutation operators P^{σ}_{12} and P^{λ}_{12} interchange spin and color labels of the spinors in the two bases. Thus the internal symmetry part of the matrix elements in (2.17) can be evaluated in terms of the complete set of operators

$$P^{\lambda}_{12}P^{\sigma}_{12},\quad P^{\lambda}_{12}\sigma_1^3\sigma_2^3,\quad P^{\lambda}_{12},\quad P^{\sigma}_{12},\quad \sigma_1{}^3\sigma_2{}^3,\quad I\ . \tag{A2}$$

These, of course, are multiplied by the quark creation and annihilation operators which depend, in addition, on the spatial orbitals. The computation proceeded by considering one by one the six-quark terms in the definition of the state (3.4). Since the operators (2.17) with the replacements (A2) merely had the effect of rearranging orbital, spin, and color labels with a particular weighting, it was then a straightforward bookkeeping matter to compute the inner product of the rearranged term with the full configuration and to tabulate the sum for all of the six-quark terms. The results are given in Sec. III and Table I.

The following consistency checks may be applied to the results:

(i) For general values of μ, interchanging the roles of S and A is equivalent to replacing $\mu \to 1/\mu$ in all terms, including in the normalization factor N. This condition equates coefficients of μ^n to coefficients of μ^{6-n} between the pairs

$$(C_{Sz}, C_{Az}),\ (C_{S\perp}, C_{A\perp}),\ (n_S, n_A)\ ,$$

and internally in all other terms in (3.6). When $\mu = 1$ it follows that

$$C_{Sz} = C_{Az},\quad C_{S\perp} = C_{A\perp}\ . \tag{A3}$$

(ii) Because the state is a color singlet, the color Casimir operator has the value

$$\langle (b_S^{\dagger}\lambda^a b_S + b_A^{\dagger}\lambda^a b_A)^2 \rangle = 0\ . \tag{A4}$$

No normal ordering is intended here. Using symmetry properties under $S \leftrightarrow A$ it can be shown that

$$\begin{aligned}\langle b_S^{\dagger}\lambda^a b_S b_S^{\dagger}\lambda^a b_S\rangle &= \langle b_A^{\dagger}\lambda^a b_A b_A^{\dagger}\lambda^a b_A\rangle \\ &= -\langle b_A^{\dagger}\lambda^a b_A b_S^{\dagger}\lambda^a b_S\rangle\ .\end{aligned} \tag{A5}$$

This result, used in (2.16), ensures that only the difference in the electric fields and charge densities for the S-S and A-A transitions appears in the expression for the energy.

(iii) In the limit $\mu = 0$ the six quarks are all in the S orbital and the results of Ref. 7 should hold. In particular

$$\begin{aligned} &n_S = 6\ , \\ &C_{Sz} + C_{S\perp} = -\tfrac{16}{3}\ ,\end{aligned} \tag{A6}$$

and all other coefficients vanish. The latter identity follows since the sum of the two coefficients gives the expectation value of $30\lambda_1^a\lambda_2^a\vec{\sigma}_1\cdot\vec{\sigma}_2$ as computed by Ref. 7.

(iv) In the limit $\mu = 1$ the six quarks divide into two triplets with quantum numbers of nucleons, each in orthogonal orbitals. The following identities must hold in order that the computation reproduce the result for two nucleons:

$$n_S = n_A = 3\ , \tag{A7a}$$

$$\begin{aligned}&C_{Sz} + C_{S\perp} + C_{SAz} + C_{SA\perp} + C_{Xz0} + C_{X\perp 0} \\ &\quad + C_{Xzd} + C_{X\perp d} + C_{Az} + C_{A\perp} = 2\times 16\ ,\end{aligned} \tag{A7b}$$

$$C_{X0} + C_{Xd} + 6(\tfrac{16}{3}) = 0\ . \tag{A7c}$$

The second identity follows since the combination reproduces the sum of the expectation of $6\lambda_1^a\lambda_2^a\vec{\sigma}\cdot\vec{\sigma}_2$ on each "nucleon". The third identity follows from the color-singlet property of the two triplets.

(v) When $\mu = 1$ further identities follow from the color-singlet property of the triplets. If we write (suppressing internal-symmetry labels)

$$b_L = b_A - b_S,\quad b_R = b_A + b_S$$

then a single gluon cannot be exchanged between the two "nucleons":

$$\begin{aligned}&\langle : b_L^{\dagger}\lambda^a\sigma^3 b_L b_R^{\dagger}\lambda^a\sigma^3 b_R : \rangle = 0\ , \\ &\langle : b_L^{\dagger}\lambda^a\sigma^{\perp} b_L b_R^{\dagger}\lambda^a\sigma^{\perp} b_R : \rangle = 0\ ,\end{aligned}$$

whence it follows that for $\mu = 1$

$$\begin{aligned}&C_{Sz} + C_{Az} + C_{SAz} - C_{Xzd} - C_{Xz0} = 0\ , \\ &C_{S\perp} + C_{A\perp} + C_{SA\perp} - C_{X\perp d} - C_{X\perp 0} = 0\ .\end{aligned}$$

We do not claim to have found an exhaustive list of identities, but those presented here served as a useful consistency check for the computed results.

---

*This work is supported in part through funds provided by ERDA under Contract No. EY-76-C-02-3069.

†Work supported in part by the A. P. Sloan Foundation.

[1]H. Yukawa, Proc. Phys. Math. Soc. Jpn. 17, 48 (1935).

[2]Rather than attempting a complete bibliography of one- and two-meson exchange potentials we mention a few representative examples: R. A. Bryan and B. L. Scott, Phys. Rev. 177, 1435 (1969); T. Ueda and A. E. S. Green, *ibid.* 174, 1304 (1968). In a more rigorous vein: M. H. Partovi and E. L. Lomon, Phys. Rev. D 2, 1999 (1970). The use of dispersion relations in connection with potential models and multiple-meson exchange is discussed by G. E. Brown and A. D. Jackson, *The Nucleon-Nucleon Interaction* (North-Holland, Amsterdam, 1976); and R. Vinh Mau, Institut de Physique Nucleaire, Report No. IPNO/TH 77-14, 1977 (unpub-

lished), and references therein.

[3]Among the more phenomenological approaches are these: M. Taketani, S. Nakamura, and M. Sasaki, Prog. Theor. Phys. 6, 581 (1951); T. Hamada and I. D. Johnston, Nucl. Phys. 34, 382 (1962); K. E. Lassila *et al.*, Phys. Rev. 126, 881 (1967); R. V. Reid, Ann. Phys. (N.Y.) 50, 411 (1968).

[4]A. Chodos, R. L. Jaffe, K. Johnson, and C. B. Thorn, Phys. Rev. D 10, 2599 (1974).

[5]Interest in quark models and bag models for the two-nucleon interaction has been growing in recent months. Some recent references are these: G. T. Fairley and E. J. Squires, Nucl. Phys. B93, 56 (1975); V. A. Matveev and Paul Sorba, Fermilab Report No. Fermilab-Pub 77/36-THY, 1977 (unpublished); Yu. F. Smirnov and Yu. M. Tchuvilsky, Moscow State University report, 1977 (unpublished). None of these works presents a detailed quantitative analysis. A more closely related work is that of David A. Liberman [Phys. Rev. D 16, 1542 (1977)], a calculation in the nonrelativistic quark model with an oscillator potential with color symmetry. No binding occurs in the deuteron channel, although it is found to be less repulsive than other channels.

[6]Pion exchange might be introduced along the lines proposed by A. Chodos and C. B. Thorn, Phys. Rev. D 12, 2733 (1975).

[7]T. DeGrand, R. L. Jaffe, K. Johnson, and J. Kiskis, *ibid.* 12, 2060 (1975).

[8]M. Born and J. R. Oppenheimer, Ann. Phys. 84, 457 (1927).

[9]We have in mind the generator coordinate method. See D. L. Hill and J. A. Wheeler, Phys. Rev. 89, 1102 (1953); J. J. Griffin and J. A. Wheeler, *ibid.* 108, 311 (1957).

[10]C. DeTar, preceding paper, Phys. Rev. D 17, 302 (1978), referred to hereafter as I. The reader will note that two new diagrams are needed in the six-quark calculation that did not appear in I, namely, those of Fig. 1(e) and 1(f).

[11]For a brief account of the use of Young tableaux, see for example, A. Bohr and B. R. Mottelson, *Nuclear Structure* (Benjamin, New York, 1969), Vol. I, p. 104ff. The reader unfamiliar with Young tableaux may skip the first two paragraphs of Sec. II.

[12]R. Balian and C. Bloch, Ann. Phys. (N.Y.) 60, 401 (1970) give a multiple reflection expansion for the cavity propagator which was applied to the fermion-bag propagator by R. L. Jaffe and A. Patrascioiu, Phys. Rev. D 12, 1314 (1975).

[13]The cavity fermion and gluon propagators contain the free-field singularity at short distance. It is felt that the presence of these singularities makes the summation over intermediate cavity modes converge slowly. In the covariant gauge the free-field singularity has a zero expectation value on the cavity eigenfunctions, and so is eliminated. Thus it was hoped that in the covariant gauge the series would converge more rapidly than in others. I am indebted to Ken Johnson for discussions on this approach.

[14]Of other static nucleon parameters of possible relevance to the two-nucleon interaction, the magnetic-dipole moment of the proton is computed in Ref. 7 and found to be too small ($2M_p\mu_p = 1.9$) compared to the experimental value (2.79). Some improvement has been reported when quark-antiquark pairs are included. See J. F. Donoghue and E. Golowich, Phys. Rev. D 15, 3421 (1977). We do not consider introducing such pairs in the present calculation.

[15]This effect could also be due to the restriction to the two lowest cavity modes—adding higher orbitals could permit a more localized three-quark cluster at smaller separations.

[16]In Figs. 3 and 10 the one-pion-exchange potential is plotted for the $I=0$ two-nucleon state with spins aligned in parallel along the separation radius, i.e., with $\vec{\sigma}_1 \cdot \vec{\sigma}_2 = 1$ and $S_{12} = 2$ in the usual notation. [See, e.g., G. Breit, Rev. Mod. Phys. 34, 766 (1962).] The potential is plotted as though $\delta \equiv r_{12}$ in Fig. 3 and $Q \equiv r_{12}^2$ in Fig. 10, where r_{12} is the internucleon separation.

[17]G. B. West, Phys. Rev. Lett. 37, 1454 (1976).